

This is the peer reviewed version of the following article:

BLOOD MICROBIOME IS ASSOCIATED WITH CHANGES IN PORTAL HYPERTENSION AFTER SUCCESSFUL DIRECT-ACTING ANTIVIRAL THERAPY IN PATIENTS WITH HCV-RELATED CIRRHOSIS

Ana Virseda-Berdices, Oscar Brochado-Kith, Cristina Díez, Victor Hontañon, Juan Berenguer, Juan González-García, David Rojo, Amanda Fernández-Rodríguez, Luis Ibañez-Samaniego, Elba Llop-Herrera, Antonio Olveira, Leire Perez-Latorre, Coral Barbas, Marta Rava, Salvador Resino, María Angeles Jiménez-Sousa, on behalf of the ESCORIAL Study Group, Blood microbiome is associated with changes in portal hypertension after successful direct-acting antiviral therapy in patients with HCV-related cirrhosis, *Journal of Antimicrobial Chemotherapy*, Volume 77, Issue 3, March 2022, Pages 719–726.

which has been published in final form at:

<https://doi.org/10.1093/jac/dkab444>

1 **Title page**

2 **Type of manuscript:** Original Article

3 **Title:** Blood microbiome is associated with changes in portal hypertension after successful
4 direct-acting antiviral therapy in patients with HCV-related cirrhosis

5 **Running head:** Blood microbiome, HVPG, and HCV therapy

6 **Authors:** Ana VIRSEDA-BERDICES ^{1¥}; Oscar BROCHADO-KITH ^{1¥}; Cristina DÍEZ ^{2,3}, Victor
7 HONTAÑÓN ^{4,5}; Juan BERENGUER ^{2,3}; Juan GONZÁLEZ-GARCÍA ^{4,5}; David ROJO ⁶; Amanda
8 FERNÁNDEZ-RODRÍGUEZ ¹; Luis IBAÑEZ-SAMANIEGO ⁷; Elba LLOP-HERRERA ⁸; Antonio
9 OLVEIRA ⁹; Leire PEREZ-LATORRE^{3,4}; Coral BARBAS ⁶; Marta RAVA ^{10†}; Salvador RESINO ^{1+*};
10 María Angeles JIMÉNEZ-SOUSA ¹⁺ on behalf of the ESCORIAL Study Group[§].

11 (¥), The authors contributed equally to this work.

12 (†), The authors contributed equally to this work.

13 (§), Members are listed in the Acknowledgements section.

14

15 **Authors' Affiliations:**

16 (1) Unidad de Infección Viral e Inmunidad, Centro Nacional de Microbiología (CNM), Instituto
17 de Salud Carlos III (ISCIII), Majadahonda, Madrid, Spain.

18 (2) Unidad de Enfermedades Infecciosas/VIH; Hospital General Universitario "Gregorio
19 Marañón", Madrid, Spain.

20 (3) Instituto de Investigación Sanitaria Gregorio Marañón (IiSGM), Madrid, Spain.

21 (4) Servicio de Medicina Interna-Unidad de VIH. Hospital Universitario La Paz. Madrid, Spain.

22 (5) Instituto de Investigación Sanitaria La Paz (IdiPAZ). Madrid, Spain.

23 (6) Centre for Metabolomics and Bioanalysis (CEMBIO), Department of Chemistry and
24 Biochemistry, Facultad de Farmacia, Universidad San Pablo-CEU, CEU Universities, Urbanización
25 Montepríncipe, 28660 Boadilla del Monte. Madrid Spain.

26 (7) Servicio de Aparato Digestivo, Hospital General Universitario "Gregorio Marañón", Madrid,
27 Spain.

28 (8) Departamento de Gastroenterología; Hospital Universitario Puerta de Hierro-Majadahonda;
29 Majadahonda, Madrid; Spain.

30 (9) Servicio de Aparato Digestivo, Hospital Universitario La Paz, Madrid, Spain

31 (10) Unidad de la Cohorte de la Red de Investigación en Sida (CoRIS). Centro Nacional de
32 Epidemiología (CNE), Instituto Carlos III (ISCIII), Madrid, Spain.

33
34
35
36
37
38
39
40
41
42
43
44
45
46
47
48
49
50
51
52
53
54
55
56
57
58
59
60
61
62
63

*** Corresponding author:** Salvador Resino; Centro Nacional de Microbiología, Instituto de Salud Carlos III; Carretera Majadahonda- Pozuelo, Km 2.2; 28220 Majadahonda (Madrid); Telf.: +34 918 223 266; Fax: +34 918 223 269; e-mail: sresino@isciii.es

Abstract

Background: Patients with a significant decrease in hepatic venous pressure gradient (HVPG) have a considerable reduction of liver complications and higher survival after hepatitis C virus (HCV) eradication. We aimed to evaluate the association between the baseline blood microbiome and the changes in HVPG after successful direct-acting antiviral (DAA) therapy in patients with HCV-related cirrhosis.

Methods: We performed a prospective study in 32 cirrhotic patients (21 HIV positive) and clinically significant portal hypertension (HVPG \geq 10 mmHg). Patients were assessed at baseline and 48 weeks after HCV treatment completion. The clinical endpoint was to decrease \geq 20% in HVPG or HVPG <12 mmHg at the end of follow-up. Bacterial 16S ribosomal DNA was sequenced using MiSeq Illumina technology, inflammatory plasma biomarkers by ProcartaPlex immunoassays, and metabolome by GC-MS.

Results: During the follow-up, 47% of patients reached the clinical endpoint. Those patients had at baseline a higher relative abundance of *Corynebacteriales* and *Diplorickettsiales* orders, *Diplorickettsiaceae* family, *Corynebacterium* and *Aquicella* genus, and *Undibacterium parvum* specie; and lower of *Oceanospirillales* and *Rhodospirillales* orders, *Halomonadaceae* family, and *Massilia* genus compared to those who did not achieve the clinical endpoint according to the LEfSe algorithm. *Corynebacteriales* and *Massilia* were consistently found within the 10 bacterial taxa with the highest differential abundance between groups. Additionally, the relative abundance of *Corynebacteriales* order was inversely correlated with IFN-gamma, IL-17A, and TNF-alpha levels and *Massilia* genus with glycerol and lauric acid.

Conclusions: Baseline-specific bacterial taxa are related to HVPG decrease in patients with HCV-related cirrhosis after successful DAA therapy.

64 **Introduction**

65 Globally, an estimated 71·million individuals have hepatitis C virus (HCV) infection,¹ the
66 leading cause of chronic liver disease. In the absence of antiviral therapy, about 5–20% of
67 patients with chronic hepatitis C develop cirrhosis, a disease that supposes a significant risk
68 for liver failure, hepatocellular carcinoma, and death.²

69 The introduction of direct-acting antivirals (DAAs) has revolutionized HCV therapy, with
70 excellent antiviral efficacy and very high cure rates.³ However, it has been described that
71 portal hypertension does not reverse in a significant number of patients who achieve
72 sustained virological response (SVR), indicating a persistent risk of progression and death.⁴
73 Portal hypertension is a severe complication of chronic liver diseases, responsible for most
74 clinical outcomes of cirrhosis.⁵ Hepatic vein catheterization with the hepatic venous pressure
75 gradient (HVPG) measurement is currently the most accurate method to assess the presence
76 and severity of portal hypertension and the best available predictor of liver-related outcomes.
77 In response to therapy, patients with a decrease in HVPG $\geq 20\%$ or a value of HVPG < 12 mmHg
78 are defined as responders,⁶ having a considerable reduction of complications and higher
79 survival.

80 Numerous studies have suggested a relevant influence of bacterial translocation in the
81 development of liver diseases related to various viral hepatitis and the pathogenesis and
82 complications of cirrhosis.^{7,8} Likewise, recent data show that bacteria in the blood can play an
83 essential role in the pathogenesis of diseases.⁹⁻¹³ Concerning liver diseases, compositional and
84 functional changes in the blood microbiome have been described in liver fibrosis and
85 cirrhosis. In this regard, Lelouvier *et al.* found a correlation between blood 16S ribosomal
86 DNA (rDNA) concentration and liver fibrosis in obese patients.¹⁴ Santiago *et al.* described an
87 alteration of the serum microbiome composition in cirrhotic patients with ascites.¹⁵ Traykova
88 *et al.* found a higher number of bacterial species and total bacterial DNA in the blood of a
89 cirrhotic cohort compared to healthy individuals,¹⁶ and Alvarez-Silva *et al.* suggested the
90 existence of a relationship between systemic inflammation and microbiota composition in
91 blood among decompensated cirrhotic patients.¹⁷ However, no previous studies have
92 described the role of the blood microbiome on the development or evolution of HCV-
93 associated liver disease. Furthermore, metabolomics studies looking at pathogen and damage-
94 associated molecular patterns and endotoxins have shown a clear correlation to the
95 microbiota, supporting the relationship between dysbiotic microbiota and systemic
96 inflammation.¹⁸

97 Therefore, since there are no data on blood microbiome in patients with HCV-related cirrhosis
98 after HCV eradication by DAA therapy, this study aimed to evaluate the influence of the blood
99 microbiome at baseline on the changes in HVPG after successful DAA therapy in patients with
100 HCV-related cirrhosis. In addition, we integrated microbiome data with the use of
101 metabolomics and inflammatory markers.

102

103 **Materials and methods**

104 **Study subjects**

105 We performed a multicenter prospective study in patients with advanced HCV-related
106 cirrhosis from the cohort ESCORIAL (see **Acknowledgements section**) enrolled in Madrid,
107 Spain, from January 2015 to June 2016. All participants gave written informed consent to
108 participate in the study. This study was conducted following the Declaration of Helsinki and
109 received the approval of the Research Ethics Committee of the Instituto de Salud Carlos III
110 (CEI41_2014, CEI42_2020).

111 The selection criteria were: 1) active HCV infection confirmed by PCR; 2) advanced cirrhosis
112 defined by any of the following criteria: i) prior history of liver decompensation (ascites,
113 bleeding esophageal varices, hepatic encephalopathy); ii) liver stiffness ≥ 25 kPa, and iii)
114 Child-Turcotte-Pugh score ≥ 7); 3) clinically significant portal hypertension defined as an
115 HVPG ≥ 10 mmHg; 4) initiation of all-oral DAA therapy and achieving an SVR. HIV/HCV-
116 coinfecting patients had undetectable plasma HIV viral load (< 50 copies/mL) and stable
117 antiretroviral therapy for more than six months.

118 **Samples and clinical data**

119 From each patient, 30-40 mL of whole blood was collected in ethylenediaminetetraacetic acid
120 tubes. Aliquots of whole blood and plasma samples obtained by centrifugation were stored
121 frozen (-80°C) in the HIV BioBank (<http://hivhgmbiobank.com/?lang=en>) until use. Baseline
122 epidemiological, clinical, and virological variables were recorded prospectively using an
123 online form within each center. HVPG was calculated by the difference between wedged
124 hepatic venous pressure and free hepatic venous pressure at baseline and 48 weeks after HCV
125 treatment completion, following well-established recommendations.¹⁹ The clinical endpoint
126 was to achieve a decrease $\geq 20\%$ in HVPG or an HVPG < 12 mmHg 48 weeks after completing
127 HCV treatment.

128 **Blood microbiome**

129 As previously described, DNA was extracted from 50 µl of each blood sample using an
130 optimized tissue-specific technique.²⁰⁻²² Library preparation was performed by two-step PCR
131 amplification using 16S universal primers targeting the V3–V4 region of the bacterial 16S
132 rDNA, as described previously.²³ For each sample, a sequencing library was generated by
133 adding sequencing adapters (full description in **Supplementary data 1**). The detection of the
134 sequencing fragments was performed using MiSeq Illumina technology. DNA extraction and
135 16S rDNA sequencing were performed in a strictly controlled environment by Vaiomer
136 (Toulouse, France) with a previously described protocol.^{20, 22, 23}

137 The targeted metagenomic sequences from microbiota were analyzed using the
138 bioinformatics pipeline established by Vaiomer based on the Find, Rapidly, operational
139 taxonomic units (OTUs) with Galaxy Solution guidelines.²⁴ OTUs were produced via single-
140 linkage clustering using the Swarm algorithm and its adaptive sequence agglomeration.²⁴ The
141 taxonomic assignment was performed against the Silva v132 database to determine
142 taxonomic profiles (full description in **Additional File 1**). Positive and negative controls were
143 added to ensure the low impact of possible DNA contamination.

144 **Non-targeted metabolomics**

145 Plasma samples were inactivated for viruses by mixing methanol for ultra-performance liquid
146 chromatography supergradient with plasma (3:1, v/v). Next, vortexing (15 seg), maintenance
147 cold for 5 min, centrifugation (16000 g, 20 min, 4°C), and freezing at 80°C were performed
148 before the shipment of samples to the Center for Metabolomics and Bioanalysis (San Pablo-
149 CEU University, Pozuelo de Alarcón, Spain). The samples were processed for the subsequent
150 measurement by gas chromatography-mass spectrometry on the day of analysis. Quality
151 controls samples were prepared by pooling and mixing equal volumes of each corresponding
152 sample. A GC system (Agilent Technologies 7890A) was used to analyze samples injected
153 through a GC-Column DB5-MS with a pre-column (full description in **Supplementary data 1**).

154 The deconvolution and identification were performed using MassHunter Quantitative
155 Unknowns Analysis (B.07.00, Agilent), alignment with MassProfiler Professional software
156 (version 13.0, Agilent), and peak integration using MassHunter Quantitative Analysis (version
157 B.07.00, Agilent).

158 **Cytokines**

159 ProcartaPlex™ multiplex immunoassay (Bender MedSystems GmbH, Vienna, Austria) was
160 used to measure the plasma concentrations of IFN- γ , IL1- β , IL10, IL12p70, IL17A, IL2, IL4, IL6,
161 TNF- α , according to the manufacturer's specifications using a Luminex 200™ analyzer
162 (Luminex Corporation, Austin, TX, United States).

163 **Statistical analysis**

164 For the descriptive study, categorical variables were shown as absolute count (percentage),
165 and quantitative variables were expressed as median (interquartile range). Comparisons
166 between groups were carried out using the Chi-square test or Fisher's exact test for
167 categorical data and the Mann-Whitney U test for continuous variables.

168 Regarding 16S metagenomic data, we used both univariable and multivariable methods to
169 evaluate differential abundance between groups. As univariable methods, we applied: i) A
170 linear discriminative analysis (LDA) effect size (LEfSe) method algorithm (Galaxy software;
171 <https://huttenhower.sph.harvard.edu/galaxy/>) to identify the bacterial taxa with the largest
172 differences in relative abundance between groups.²⁵ Only taxa with an LDA score >2 and a
173 significance of alpha <0.05 were selected; ii) Wilcoxon test: nonparametric test to compare
174 relative abundances of bacterial taxa between groups. Also, we applied statistical methods
175 that allowed adjustment for covariates, including age, sex, and coinfection with HIV in the
176 multivariable models, in order to avoid potential confounders. In this regard, we applied: iii)
177 ALDEx2:²⁶ the relative abundances were estimated by repeated samplings from a Dirichlet
178 distribution and centered-log ratio transformed before fitting the generalized linear model
179 (via `aldex.glm`); iv) MetagenomeSeq:²⁷ a zero-inflated Gaussian model, where the count
180 distribution was modeled as a mixture of two distributions, a point mass at zero and a normal
181 distribution. Since OTUs are usually sparse, the zero counts are modeled with the former, and
182 the rest of the log-transformed counts are modeled as the latter distribution.

183 Moreover, Spearman correlation was carried out to investigate the relationship between the
184 relative abundance of significant bacterial taxa and inflammatory biomarkers and plasma
185 metabolites. Using the false discovery rate (FDR) with Benjamini and Hochberg procedure, P-
186 values were corrected for multiple testing.

187 The statistical analysis was carried out with SPSS (SPSS INC, Chicago, IL, USA) and R statistical
188 package (R Foundation for Statistical Computing, Vienna, Austria).

189

190 **Results**

191 **Characteristics of the study population**

192 **Table 1** describes the characteristics of 32 patients with advanced HCV-related cirrhosis (11
193 HCV-monoinfected and 21 HIV/HCV-coinfected). Overall, the median age was 52.9 years,
194 65.6% were men, 56% were current smokers, and 50% had a prior history of injection drug
195 use. Regarding virological aspects, 50% had previously failed interferon-based therapy, 64.5%
196 were infected with HCV-genotype 1, 65.6% were coinfecting with HIV, and 38.1% had AIDS
197 before.

198 During the follow-up, 47% of patients reached the clinical endpoint (decrease of HVPG \geq 20%
199 and/or HVPG < 12 mmHg 48 weeks after completing HCV treatment). Patients who achieved
200 the endpoint showed similar characteristics to those who did not, except for HIV coinfection
201 ($p=0.019$).

202 **Microbiome data**

203 We evaluated the differences at all taxonomic levels between endpoint groups using the LEfSe
204 algorithm (**Figure 1A**). The cladogram shows the differences at various taxonomic levels
205 starting from phylum levels at the inner circle to class, order, family, genus, and species levels
206 toward the periphery (**Figure 1B**). In this analysis, *Corynebacteriales* (LDA=3.53, $p=0.010$),
207 *Diplorickettsiaceae* (LDA=3.07, $p=0.014$), *Diplorickettsiales* (LDA=3.06, $p=0.014$),
208 *Corynebacterium* (LDA=2.96, $p=0.025$), *Aquicella* (LDA= 2.89, $p=0.005$) and *Undibacterium*
209 *parvum* (LDA=2.60, $p=0.025$) had higher relative abundance in patients who reached the
210 endpoint; while *Halomonadaceae* (LDA=2.50, $p=0.049$), *Oceanospirillales* (LDA=2.56,
211 $p=0.049$), *Rhodospirillales* (LDA=2.60, $p=0.049$), and *Massilia* (LDA=3.38, $p=0.031$) had higher
212 relative abundances in patients who not reached the endpoint. Of them, *Corynebacteriales* and
213 *Massilia* were consistently found within the 10 bacterial taxa with the highest differential
214 abundance between groups according to all the statistical methods used (LEfSe, ALDEx2,
215 MetagenomeSeq, and Wilcoxon) and also after adjustment for age, sex, and HIV coinfection in
216 multivariate methods (ALDEx2 and MetagenomeSeq), indicating that its abundances were
217 associated with the endpoint, regardless of age, sex, and HIV coinfection (**Figure 2, Table S1**).

218 **Correlation analysis**

219 **Table 2** shows the statistically significant correlations found between the bacterial taxa in the
220 blood and the plasma markers of inflammation and metabolites at baseline. Relative
221 abundance of *Corynebacteriales* order was inversely correlated with IFN- γ , IL17A and TNF- α

222 (r=-0.743, q=0.041; r=-0.430, q=0.042; r=-0.454, q=0.041, respectively) and *Massilia* genus
223 abundance was inversely correlated with glycerol and lauric acid (r=-0.541, q=0.047; r=-
224 0.585, q=0.030).

225

226

227 **Discussion**

228 We assessed for the first time the association of blood microbiome with changes in HVPG after
229 successful DAA therapy in patients with HCV-related liver cirrhosis. We found a higher
230 relative abundance of *Corynebacteriales* order at baseline in patients achieving a decrease
231 $\geq 20\%$ in HVPG or HVPG < 12 mmHg 48 weeks after completing HCV treatment. In contrast, a
232 higher relative abundance of *Massilia* genus at baseline was observed in those not achieving
233 this endpoint.

234 The presence of bacterial DNA in blood has been previously described. Specifically, blood
235 bacterial DNA has been detected in about 90% of cirrhotic patients without clinical evidence
236 of infection, suggesting that the blood microbiome could stimulate inflammatory signaling
237 pathways,¹⁶ and contribute to the pathogenesis of cirrhosis. Our study shows a higher relative
238 abundance of *Corynebacteriales* order at baseline in those patients who reached the portal
239 pressure endpoint. The *Corynebacteriales* order encompasses a group of Gram-positive
240 bacteria widely distributed in nature, including corynebacteria, nocardia, mycobacteria,
241 rhodococci, and other related microorganisms.²⁸ Our results agree with previous studies,
242 where a greater abundance of the *Corynebacteriales* order was found in patients with
243 ulcerative colitis that improved significantly after treatment of the disease,²⁹ decreasing the
244 levels of proinflammatory cytokines. However, the role of *Corynebacteriales* in liver diseases is
245 still unknown. To further explore its potential role in patients with HCV-related cirrhosis, we
246 studied its correlation with inflammatory and metabolic markers. In this context, an inverse
247 correlation between the relative abundance of *Corynebacteriales* order and plasma levels of
248 several inflammation-related biomarkers was found, being IFN- γ , IL17A, and TNF- α the most
249 significantly associated markers. Among them, elevated levels of IFN- γ are associated with
250 hepatic dysfunction in fibrosis, cirrhosis, and hepatocellular carcinoma.³⁰ Likewise, the
251 Th17/IL17 axis is involved in fibrogenesis, activation of stellate cells, and increased
252 expression of profibrotic factors in patients with HCV liver disease.³¹ Additionally, higher
253 levels of TNF- α are associated with liver disease progression and hepatocellular carcinoma.³²
254 Therefore, the favorable role of the higher relative abundance of *Corynebacteriales* order at
255 baseline could be explained by its inverse correlation with inflammatory markers previously
256 linked to liver disease progression. This supposes a highly relevant finding, but additional
257 studies would be interesting to corroborate these findings.

258 Another bacterial taxa that showed a relevant role in HVPG after achieving SVR was the
259 *Massilia* genus since a higher relative abundance of *Massilia* in blood at baseline was

260 associated with a worse evolution of portal hypertension. This bacterium was described in
261 1998 in the blood of an immunocompromised individual with cerebellar lesions.³³ However,
262 its pathogenicity was described as unknown. Since then, *Massilia* genus has been found in
263 different human fluids, such as blood, cerebrospinal fluid, bone, and eye.³³⁻³⁵ Regarding its
264 role in infectious diseases, it has been observed that the nonpathogenic bacterium *Massilia* sp.
265 can efficiently reactivate HIV-reservoir by secreting an HIV-1-reactivating protein factor
266 (HRF) in HIV-infected patients.³⁶ In our study, although HIV/HCV-coinfected patients had
267 stable antiretroviral therapy and undetectable plasma HIV viral load, the presence of *Massilia*
268 genus and the HRF secretion could have an additional unknown role on the liver disease,
269 contributing to a worse recovery after HCV eradication in this subset of patients. In addition,
270 HRF leads to a high nonsustained peak in nuclear factor kappa B (NF- κ B); however, it has not
271 been associated with increased expression of proinflammatory genes induced by NF- κ B.³⁶
272 This evidence agrees with our results since we also observed an absence of correlation
273 between the relative abundance of *Massilia* genus and inflammation-related biomarkers.

274 When we explored the relationship between *Massilia* and metabolic molecules, we found that
275 increased relative abundance of *Massilia* genus was correlated with decreased plasma levels
276 of glycerol and free fatty acids. In this setting, a metabolic effect of *Massilia* was previously
277 described. Some *Massilia* genus members have shown the capacity to degrade aromatic
278 compounds and the ability to accumulate polyhydroxyalkanoates (PHAs) as intracellular
279 granules.³⁷ Thus, the decreased level of glycerol could be due to its use for PHA production,³⁸
280 which is involved in collagen deposition and enhanced fibrosis.³⁹ On the other hand, *Massilia*
281 genus was inversely correlated with several fatty acids, such as lauric acid, palmitic acid, and
282 palmitoleic acid. However, only lauric acid remained significant after adjustment for multiple
283 comparisons. Interestingly, the monoester formed from glycerol and lauric acid, called
284 glycerol monolaurate, has been significantly associated with improved hepatic lipid
285 metabolism and antimicrobial and anti-inflammatory properties.^{40,41} In this regard, the
286 decreased levels of glycerol and lauric acid associated with a higher relative abundance of
287 *Massilia* could be contributing to the unfavorable evolution of patients with HCV-related
288 cirrhosis after successful DAA therapy.

289 Remarkably, it is essential to note that this study was carried out using a rigorous
290 contamination-aware approach. On the one hand, the high volume of blood withdrawn
291 prevents any potential contamination by needle with the skin microbiome. On the other hand,
292 negative and positive controls were added and carried over throughout the sequencing

293 pipeline to prevent any significant impact of the environment on the results. Additionally, due
294 to the variability found among different statistical methods when analyzing massive data, we
295 replicate the analysis by several statistical methods, some of them adjusting for the most
296 relevant covariates. All of these approaches provide robustness to our data.

297 Other points should be considered for a correct data interpretation. The sample size was
298 limited, which could restrict the statistical power to detect more relevant bacterial taxa
299 involved in improving portal hypertension after DAA therapy. Besides, we could not study the
300 associations separately for HCV-monoinfected and HIV/HCV- coinfecting patients due to the
301 limited sample size. Nevertheless, possible confusion with HIV coinfection was ruled out by
302 including HIV status as a covariate in multivariate models. Additionally, an important strength
303 of this study is the availability of the HVPG measurement in a prospective design, with a
304 relatively long interval from the end of the treatment to the determination of the follow-up
305 portal hemodynamic study. Besides, our research adheres to the STROBE recommendations
306 (see **Table S2**).

307 In conclusion, the higher relative abundance of *Corynebacteriales* at baseline was consistently
308 associated with achieving a decrease $\geq 20\%$ in HVPG or HVPG < 12 mmHg at 48 weeks after
309 HCV treatment completion. In contrast, the increased abundance of *Massilia* was associated
310 with worse evolution in the measurement of HVPG. These findings are the first evidence that
311 blood-specific bacterial taxa could reduce portal hypertension after achieving SVR in patients
312 with advanced HCV-related cirrhosis.

313

314 **Declarations**

315 **Transparency declarations**

316 None to declare.

317 **Originality**

318 The authors confirm that the material contained herein is entirely original.

319 **Availability of data and materials**

320 Datasets used and analyzed during the current study may be available from the corresponding
321 author upon reasonable request.

322 **Competing interests**

323 The authors declare that they have no competing interests.

324 **Funding**

325 This study was supported by grants from Instituto de Salud Carlos III (ISCIII; grant numbers
326 CP17CIII/00007 and PI18CIII/00028 to MAJS, PI14/01094 and PI17/00657 to JB,
327 PI14/01581 and PI17/00903 to JGG, and PI14CIII/00011 and PI17CIII/00003 to SR) and
328 Ministerio de Sanidad, Servicios Sociales e Igualdad (grant number EC11-241). The study was
329 also funded by the Spanish AIDS Research Network (RD16/0025/0017, RD16/0025/0018
330 and RD16CIII/0002/0002) and Centro de Investigación Biomédica en Red (CIBER) en
331 Enfermedades Infecciosas (CB21/13/00044). JB is an investigator from the Programa de
332 Intensificación de la Actividad Investigadora en el Sistema Nacional de Salud (I3SNS), Refs
333 INT16/00100. CB and DR acknowledge funding from the Ministerio de Ciencia, Innovación y
334 Universidades (RTI2018-095166-B-I00). AFR, MAJS and MR are Miguel Servet researchers
335 supported and funded by ISCIII (grant numbers: CP14CIII/00010 to AFR, CP17CIII/00007 to
336 MAJS and CP19CIII/00002 to MR).

337 **Authorship contribution**

338 Funding body: MAJS and SR.

339 Study concept and design: MAJS.

340 Patients' selection and clinical data acquisition: CD, VH, JB, JGG, LIS, ELH, AO, LPL.

341 Sample preparation and biomarker analysis: OBK, AVB, AFR, DR, CB.

342 Statistical analysis and interpretation of data: OBK, AVB, MR, MAJS.

343 Writing of the manuscript: MAJS.

344 Critical revision of the manuscript for relevant intellectual content: JB, JGG, DR, CB, AFR, MR,
345 SR.

346 Supervision and visualization: MR, SR, MAJS.

347 All authors approved the final version of the article.

348 **Acknowledgments**

349 This study would not have been possible without the collaboration of all the patients, medical
350 and nursery staff, and data managers who have taken part in the project. We want to
351 particularly acknowledge the support of the HIV BioBank, which is integrated into the Spanish
352 AIDS Research Network and all collaborating Centres, for the generous contribution with
353 clinical samples for the present work. The HIV BioBank, is supported by Instituto de Salud
354 Carlos III, Spanish Health Ministry (Grant nº RD06/0006/0035, RD12/0017/0037 and
355 RD16/0025/0019) as part of the Plan Nacional R + D + I and cofinanced by ISCIII-
356 Subdirección General de Evaluación y el Fondo Europeo de Desarrollo Regional (FEDER)". The
357 RIS Cohort (CoRIS) is funded by the Instituto de Salud Carlos III through the Red Temática de
358 Investigación Cooperativa en SIDA (RIS C03/173, RD12/0017/0018 and RD16/0002/0006)
359 as part of the Plan Nacional R+D+I and cofinanced by ISCIII-Subdirección General de
360 Evaluacion and the Fondo Europeo de Desarrollo Regional (FEDER). The following hospitals
361 and members participate in the ESCORIAL study group: i) **Hospital General Universitario**
362 **Gregorio Marañón** (Madrid, Spain): Cristina Díez, Luis Ibáñez, Leire Pérez-Latorre, Diego
363 Rincón, Teresa Aldámiz-Echevarría, Vega Catalina, Pilar Miralles, Teresa Aldámiz-Echevarría,
364 Francisco Tejerina, María C Gómez-Rico, Esther Alonso, José M Bellón, Rafael Bañares, and
365 Juan Berenguer; ii) **Hospital Universitario La Paz/IdiPAZ** (Madrid, Spain): José Arribas, José
366 I Bernardino, Carmen Busca, Ana Delgado, Javier García-Samaniego, Víctor Hontañón, Luz
367 Martín-Carbonero, Rafael Micán, María L Montes-Ramírez, Victoria Moreno, Antonio Olveira,
368 Ignacio Pérez-Valero, Eulalia valencia, and Juan González-García; iii) **Hospital Universitario**
369 **Puerta de Hierro** (Madrid, Spain): Elba Llop and José Luis Calleja; iv) **Hospital Universitario**
370 **Ramón y Cajal** (Madrid, Spain): Javier Martínez and Agustín Albillos; v) **Fundación**
371 **SEIMC/GeSIDA** (Madrid, Spain): Marta de Miguel, María Yllescas, and Herminia Esteban.

372

373

374

References

- 376 1. Spearman CW, Dusheiko GM, Hellard M *et al.* Hepatitis C. *Lancet* 2019; **394**: 1451-66.
- 377 2. Bruden DJT, McMahon BJ, Townshend-Bulson L *et al.* Risk of end-stage liver disease,
378 hepatocellular carcinoma, and liver-related death by fibrosis stage in the hepatitis C Alaska
379 Cohort. *Hepatology* 2017; **66**: 37-45.
- 380 3. Seifert LL, Perumpail RB, Ahmed A. Update on hepatitis C: Direct-acting antivirals.
381 *World J Hepatol* 2015; **7**: 2829-33.
- 382 4. Diez C, Berenguer J, Ibanez-Samaniego L *et al.* Persistence of Clinically Significant
383 Portal Hypertension After Eradication of Hepatitis C Virus in Patients With Advanced
384 Cirrhosis. *Clin Infect Dis.* 2020; **71**: 2726-9.
- 385 5. Berzigotti A. Advances and challenges in cirrhosis and portal hypertension. *BMC med*
386 2017; **15**: 200.
- 387 6. Bosch J, Abraldes JG, Berzigotti A *et al.* The clinical use of HVPG measurements in
388 chronic liver disease. *Nat Rev Gastroenterol Hepatol* 2009; **6**: 573-82.
- 389 7. Sandler NG, Koh C, Roque A *et al.* Host response to translocated microbial products
390 predicts outcomes of patients with HBV or HCV infection. *Gastroenterology* 2011; **141**: 1220-
391 30, 30 e1-3.
- 392 8. Jalan R, Gines P, Olson JC *et al.* Acute-on chronic liver failure. *J Hepatol* 2012; **57**: 1336-
393 48.
- 394 9. Amar J, Lelouvier B, Servant F *et al.* Blood Microbiota Modification After Myocardial
395 Infarction Depends Upon Low-Density Lipoprotein Cholesterol Levels. *J Am Heart Assoc* 2019;
396 **8**: e011797.
- 397 10. Hammad DBM, Hider SL, Liyanapathirana VC *et al.* Molecular Characterization of
398 Circulating Microbiome Signatures in Rheumatoid Arthritis. *Front Cell Infect Microbiol* 2019;
399 **9**: 440.
- 400 11. Ouaknine Krief J, Helly de Tauriers P, Dumenil C *et al.* Role of antibiotic use, plasma
401 citrulline and blood microbiome in advanced non-small cell lung cancer patients treated with
402 nivolumab. *J Immunother Cancer* 2019; **7**: 176.
- 403 12. Shah NB, Allegretti AS, Nigwekar SU *et al.* Blood Microbiome Profile in CKD : A Pilot
404 Study. *Clin J Am Soc Nephrol: CJASN* 2019; **14**: 692-701.
- 405 13. Whittle E, Leonard MO, Gant TW *et al.* Multi-Method Molecular Characterisation of
406 Human Dust-Mite-associated Allergic Asthma. *Sci Rep* 2019; **9**: 8912.
- 407 14. Lelouvier B, Servant F, Paisse S *et al.* Changes in blood microbiota profiles associated
408 with liver fibrosis in obese patients: A pilot analysis. *Hepatology* 2016; **64**: 2015-27.
- 409 15. Santiago A, Pozuelo M, Poca M *et al.* Alteration of the serum microbiome composition in
410 cirrhotic patients with ascites. *Sci Rep* 2016; **6**: 25001.

- 411 16. Traykova D, Schneider B, Chojkier M *et al.* Blood Microbiome Quantity and the
412 Hyperdynamic Circulation in Decompensated Cirrhotic Patients. *PLoS One* 2017; **12**:
413 e0169310.
- 414 17. Alvarez-Silva C, Schierwagen R, Pohlmann A *et al.* Compartmentalization of Immune
415 Response and Microbial Translocation in Decompensated Cirrhosis. *Front Immunol* 2019; **10**:
416 69.
- 417 18. Acharya C, Bajaj JS. Altered Microbiome in Patients With Cirrhosis and Complications.
418 *Clin Gastroenterol Hepatol* 2019; **17**: 307-21.
- 419 19. Groszmann RJ, Wongcharatrawee S. The hepatic venous pressure gradient: anything
420 worth doing should be done right. *Hepatology* 2004; **39**: 280-2.
- 421 20. Anhe FF, Jensen BAH, Varin TV *et al.* Type 2 diabetes influences bacterial tissue
422 compartmentalisation in human obesity. *Nat Metab* 2020; **2**: 233-42.
- 423 21. Paise S, Valle C, Servant F *et al.* Comprehensive description of blood microbiome from
424 healthy donors assessed by 16S targeted metagenomic sequencing. *Transfusion* 2016; **56**:
425 1138-47.
- 426 22. Schierwagen R, Alvarez-Silva C, Servant F *et al.* Trust is good, control is better:
427 technical considerations in blood microbiome analysis. *Gut* 2020; **69**: 1362-3.
- 428 23. Lluch J, Servant F, Paise S *et al.* The Characterization of Novel Tissue Microbiota Using
429 an Optimized 16S Metagenomic Sequencing Pipeline. *PLoS One* 2015; **10**: e0142334.
- 430 24. Escudie F, Auer L, Bernard M *et al.* FROGS: Find, Rapidly, OTUs with Galaxy Solution.
431 *Bioinformatics* 2018; **34**: 1287-94.
- 432 25. Segata N, Izard J, Waldron L *et al.* Metagenomic biomarker discovery and explanation.
433 *Genome Biol* 2011; **12**: R60.
- 434 26. Fernandes AD, Reid JN, Macklaim JM *et al.* Unifying the analysis of high-throughput
435 sequencing datasets: characterizing RNA-seq, 16S rRNA gene sequencing and selective growth
436 experiments by compositional data analysis. *Microbiome* 2014; **2**: 15.
- 437 27. Paulson JN, Stine OC, Bravo HC *et al.* Differential abundance analysis for microbial
438 marker-gene surveys. *Nat Methods* 2013; **10**: 1200-2.
- 439 28. de Sousa-d'Auria C, Constantinesco-Becker F, Constant P *et al.* Genome-wide
440 identification of novel genes involved in Corynebacteriales cell envelope biogenesis using
441 *Corynebacterium glutamicum* as a model. *PLoS One* 2020; **15**: e0240497.
- 442 29. Yang H, Gan D, Li Y *et al.* Quyushengxin Formula Causes Differences in Bacterial and
443 Phage Composition in Ulcerative Colitis Patients. *Evid Based Complement Alternat Med : eCAM*
444 2020; **2020**: 5859023.
- 445 30. Attallah AM, El-Far M, Zahran F *et al.* Interferon-gamma is associated with hepatic
446 dysfunction in fibrosis, cirrhosis, and hepatocellular carcinoma. *J Immunoassay immunochem*
447 2016; **37**: 597-610.

- 448 31. Paquissi FC. Immunity and Fibrogenesis: The Role of Th17/IL-17 Axis in HBV and HCV-
449 induced Chronic Hepatitis and Progression to Cirrhosis. *Front Immunol* 2017; **8**: 1195.
- 450 32. Aroucha DC, do Carmo RF, Moura P *et al.* High tumor necrosis factor-alpha/interleukin-
451 10 ratio is associated with hepatocellular carcinoma in patients with chronic hepatitis C.
452 *Cytokine* 2013; **62**: 421-5.
- 453 33. La Scola B, Birtles RJ, Mallet MN *et al.* *Massilia timonae* gen. nov., sp. nov., isolated from
454 blood of an immunocompromised patient with cerebellar lesions. *J Clin Microbiol* 1998; **36**:
455 2847-52.
- 456 34. Kampfer P, Lodders N, Martin K *et al.* *Massilia oculi* sp. nov., isolated from a human
457 clinical specimen. *Int J Syst Evol Microbiol* 2012; **62**: 364-9.
- 458 35. Lindquist D, Murrill D, Burran WP *et al.* Characteristics of *Massilia timonae* and
459 *Massilia timonae*-like isolates from human patients, with an emended description of the
460 species. *J Clin Microbiol* 2003; **41**: 192-6.
- 461 36. Wolschendorf F, Duverger A, Jones J *et al.* Hit-and-run stimulation: a novel concept to
462 reactivate latent HIV-1 infection without cytokine gene induction. *J Virol* 2010; **84**: 8712-20.
- 463 37. Rodriguez-Diaz M, Cerrone F, Sanchez-Peinado M *et al.* *Massilia umbonata* sp. nov., able
464 to accumulate poly-beta-hydroxybutyrate, isolated from a sewage sludge compost-soil
465 microcosm. *Int J Syst Evol Microbiol* 2014; **64**: 131-7.
- 466 38. Moita R, Freches A, Lemos PC. Crude glycerol as feedstock for polyhydroxyalkanoates
467 production by mixed microbial cultures. *Water Res* 2014; **58**: 9-20.
- 468 39. Gumel AM, Razaif-Mazinah MR, Anis SN *et al.* Poly (3-hydroxyalkanoates)-co-(6-
469 hydroxyhexanoate) hydrogel promotes angiogenesis and collagen deposition during
470 cutaneous wound healing in rats. *Biomed Mater* 2015; **10**: 045001.
- 471 40. Zhao M, Jiang Z, Cai H *et al.* Modulation of the Gut Microbiota during High-Dose
472 Glycerol Monolaurate-Mediated Amelioration of Obesity in Mice Fed a High-Fat Diet. *mBio*
473 2020; **11**:e00190-20.
- 474 41. Schlievert PM, Kilgore SH, Seo KS *et al.* Glycerol Monolaurate Contributes to the
475 Antimicrobial and Anti-inflammatory Activity of Human Milk. *Sci Rep* 2019; **9**: 14550.
476

478
479
480
481
482

Tables

Table 1. Clinical and epidemiological characteristics of patients with advanced HCV-related cirrhosis stratified by reaching a decrease in HVPG $\geq 20\%$ and/or HVPG <12 mmHg 48 weeks after completing HCV treatment.

Variables	All patients	Endpoint not achieved	Endpoint achieved	<i>p</i>
No.	32	17 (53.1%)	15 (46.9%)	-
Age (years)	52.9 (49.9-55.2)	53.4 (52.1-59.7)	52.2 (47.9-55.0)	0.136
Gender (male)	21 (65.6%)	11 (64.7%)	10 (66.7%)	0.907
BMI (kg/m ²)	25.1 (22.9-27.9)	25.4 (22.9-28.4)	24.5 (23.4-27.4)	0.550
Smoker				
Never	8 (25%)	4 (23.5%)	4 (26.7%)	0.952
Previous (>6m)	6 (18.8%)	3 (17.6%)	3 (20.0%)	
Current	18 (56.3%)	10 (58.8%)	8 (53.3%)	
High alcohol intake (>50 g/day)				
Never	18 (56.3%)	11 (64.7%)	7 (46.7%)	0.250
Previous (>6m)	12 (37.5%)	6 (35.3%)	6 (40.0%)	
Current	2 (6.3%)	0 (0%)	2 (13.3%)	
History of IDU	16 (50%)	6 (35.3%)	10 (66.7%)	0.077
Previous anti-HCV therapy	16 (50%)	10 (58.8%)	6 (40.0%)	0.288
Treatment with statins	4 (12.5%)	1 (5.9%)	3 (20.0%)	0.319
Other liver markers				
CPT score	5 (5-6)	6 (5-7)	5 (5-5)	0.095
MELD score	8 (7-12)	10 (7-12)	8 (7-10)	0.658
LSM	34.8 (20.8-48.4)	34.3 (21.1-48.8)	35.3 (16.9-48.0)	0.734
HVPG	16.5 (14.8-18.0)	17.0 (15.0-18.0)	16.0 (13.5-17.5)	0.315
HCV markers				
HCV genotype (n=31)				
1	20 (64.5%)	12 (75.0%)	8 (53.3%)	0.329
2	1 (3.2%)	1 (6.3%)	0 (0%)	
3	4 (12.9%)	1 (6.3%)	3 (20.0%)	
4	6 (19.4%)	2 (12.5%)	4 (26.7%)	
Log ₁₀ HCV-RNA (IU/mL)	5.9 (5.5-6.6)	5.8 (5.4-6.2)	6.5 (5.7-6.8)	0.057
HCV-RNA > 850,000 IU/mL	16 (50.0%)	7 (41.2%)	9 (60.0%)	0.288
HIV markers				
HIV coinfection	21 (65.6%)	8 (47.1%)	13 (86.7%)	0.019
Previous AIDS (n=21)	8 (38.1%)	5 (62.5%)	3 (23.1%)	0.164
Nadir CD4 ⁺ T cells (n=19)	130 (54-319)	83 (38-152)	207 (70-382)	0.148
Nadir CD4 ⁺ T cells <200 cells/mm ³ (n=19)	12 (63.2%)	7 (87.5%)	5 (45.5%)	0.147
Baseline CD4 ⁺ T cells	490 (234-719)	288 (238-491)	712 (233-827)	0.218
Baseline CD4 ⁺ T cells <500 cells/mm ³	12 (57.1%)	7 (87.5%)	5 (38.5%)	0.067
Antiretroviral therapy				
NRTI+NNRTI	2 (9.5%)	1 (12.5%)	1 (7.7%)	0.763
NRTI+II	11 (52.4%)	3 (37.5%)	8 (61.5%)	
NRTI+PI	3 (14.3%)	1 (12.5%)	2 (15.4%)	
PI+II+NNRTI/MVC	2 (9.5%)	1 (12.5%)	1 (7.7%)	
Others	3 (14.3%)	2 (25.0%)	1 (7.7%)	

483
484
485
486
487
488
489
490

Statistics: Values are expressed as absolute number (percentage) and median (25th percentile -75th percentile). *P*-values were calculated by Chi-square test or Fisher exact test for categorical variables and the Mann-Whitney U test for continuous variables. The clinical outcome was to decrease $\geq 20\%$ in HVPG or HVPG <12 mmHg at the end of follow-up. Significant differences are shown in bold. **Abbreviations:** BMI, body mass index; 6m, 6 months; IDU, injection drug use; HCV, hepatitis C virus; HCV-RNA, HCV plasma viral load; HIV, human immunodeficiency; CPT, Child-Turcotte-Pugh; MELD, model for end-stage liver disease; LSM, liver stiffness measurement; HVPG, hepatic venous pressure gradient; AIDS, acquired

491 immune deficiency syndrome; NNRTI, non-nucleoside analogue HIV reverse transcriptase inhibitor;
492 NRTI, nucleoside analogue HIV reverse transcriptase inhibitor; PI, protease inhibitor; II, integrase
493 inhibitor, MVC, maraviroc.
494

495

496 **Table 2.** Correlation between blood significant bacterial taxa and plasma markers of
 497 inflammation and metabolites at baseline.
 498

<u>Phylum</u>	<u>Taxa</u>	<u>Plasma marker</u>	<u>rho</u>	<u>p-value</u>	<u>q-value</u>
		IFNgamma	-0.473	0.006	0.041
		IL12p70	-0.363	0.041	0.092
		IL17A	-0.430	0.014	0.042
<i>Actinobacteria</i>	<i>Corynebacteriales</i>	TNFalpha	-0.454	0.009	0.041
		Oxoproline	0.364	0.041	0.782
		Aminomalonic.acid	0.354	0.047	0.782
		Tryptophan	0.471	0.006	0.445
		Tyrosine	0.357	0.045	0.782
		Glycerol	-0.541	0.001	0.047
		Fructose/Psicose/ Sorbose/Tagatose	0.385	0.029	0.427
<i>Proteobacteria</i>	<i>Massilia</i>	Lauric acid	-0.585	<0.001	0.030
		Palmitic acid	-0.382	0.031	0.427
		Palmitoleic acid	-0.490	0.004	0.102

499

500 **Statistics:** P-values were calculated by Spearman correlation; q-values represent p-values
 501 corrected for multiple testing using the False Discovery Rate (FDR). Significant differences are
 502 shown in bold.

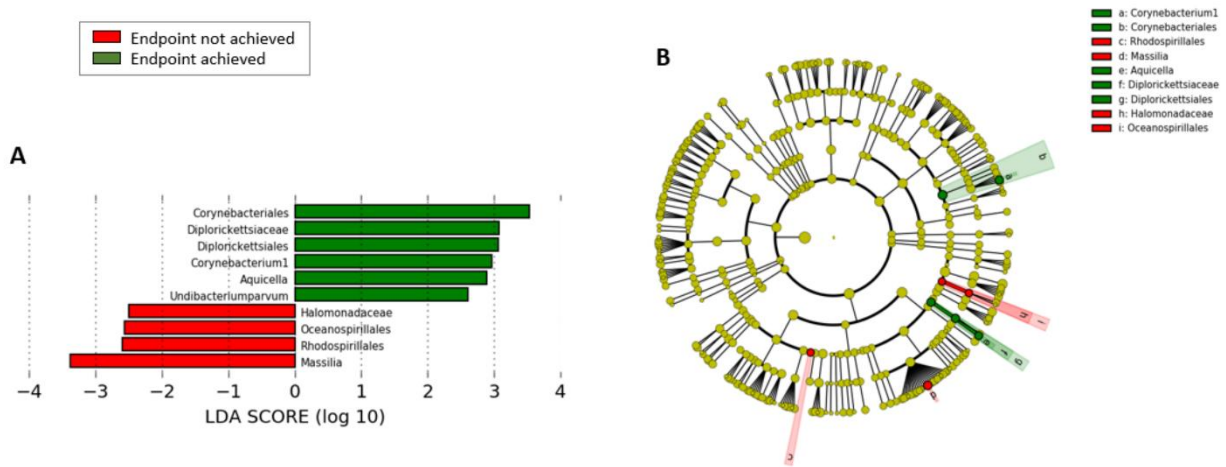
503 **Abbreviations:** IFN, interferon; IL, interleukin; p-value, level of significance; q-value, corrected
 504 level of significance.

505

506

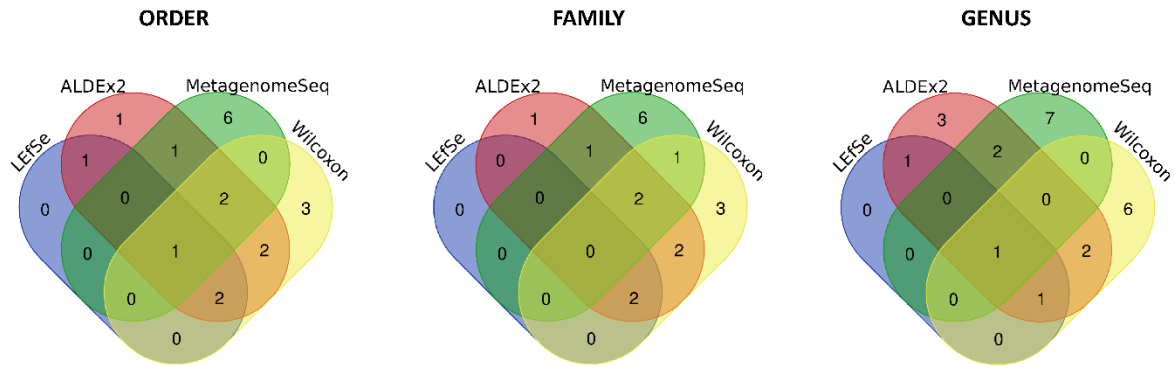
507 **Figures**

508 **Figure 1.** Different abundances of bacterial communities in blood between those patients who
 509 reached a HVPG decrease $\geq 20\%$ or HVPG $< 12\text{mmHg}$ and those who did not 48 weeks after
 510 completing HCV therapy by using LEfSe analysis. (A) Taxa enriched in patients who reached
 511 the endpoint are indicated with a positive LDA score (green), and taxa enriched in patients
 512 who did not get the endpoint with a negative LDA score (red). Only taxa meeting an LDA
 513 significant threshold two are shown. (B): Bacterial taxa that were differentially abundant in
 514 the blood microbiome using a cladogram generated from LEfSe analysis.



516 **Figure 2.** Overlapping of the ten most differentially abundant bacterial taxa identified for each
 517 statistical method using Venn diagrams and according to order, family and genus. The
 518 overlapping numbers correspond to bacterial taxa shared between different methods. The
 519 colors of the ovals correspond to the different statistical methods used: LefSe (blue), ALDEx2
 520 (red), MetagenomeSeq (green), and Wilcoxon test (yellow).

521



Methods	Order	Family	Genus
LefSe ALDEx2 MetagenomeSeq Wilcoxon	Corynebacteriales	-	Massilia
LefSe ALDEx2 Wilcoxon	Diplorickettsiales	Diplorickettsiaceae	Aquicella
LefSe ALDEx2	Rhodospirillales	Halomonadaceae	
	Oceanospirillales	-	Corynebacterium1

522 **Supplementary data**

523 **Supplementary data 1.** Additional description of the methods section.

524 **Table S1.** The ten most differentially abundant bacterial taxa obtained using ALDEx2,
525 MetagenomeSeq and Wilcoxon test, according to the taxonomic ranks of order family and
526 genus. Statistics: i) ALDEx2: estimates were obtained of differential abundance analyses
527 accounting for potential confounders (age, gender, and HIV coinfection). The relative
528 abundances were estimated by repeated samplings from a Dirichlet distribution and
529 centered-log ratio (clr) transformed before fitting the GLM model; ii) MetagenomeSeq:
530 Estimates were obtained after fitting a zero-inflated Gaussian (ZIG) model, where the count
531 distribution is modeled as a mixture of two distributions, a point mass at zero and a normal
532 distribution. Since OTUs are usually sparse, the zero counts are modeled with the former, and
533 the rest of the log-transformed counts are modeled as the latter distribution; iii) Wilcoxon
534 test: nonparametric test to compare relative abundances of bacterial taxa between groups.

535 **Table S2.** STROBE Statement—checklist of items that should be included in reports of
536 observational studies.